

***Final Draft***  
**of the original manuscript:**

Lau, S.; Rangarajan, R.; Philidet, C.; Krüger-Genge, A.; Braune, S.; Kammerer, S.; Küpper, J.; Lendlein, A.; Jung, F.:

**Effects of acrolein in comparison to its prodrug cyclophosphamide on human primary endothelial cells in vitro.**

In: Toxicology in Vitro. Vol. 62 (2020) 104685.

First published online by Elsevier: 18.10.2019

DOI: 10.1016/j.tiv.2019.104685

<https://dx.doi.org/10.1016/j.tiv.2019.104685>

## **Effects of acrolein in comparison to its prodrug cyclophosphamide on human primary endothelial cells *in vitro***

S. Lau<sup>a</sup>, R. Rangarajan<sup>a</sup>, C. Philidet<sup>a</sup>, A. Krüger-Genge<sup>a#</sup>, S. Braune<sup>a</sup>, S. Kammerer<sup>b</sup>, J.-H. Küpper<sup>b</sup>, A. Lendlein<sup>a,c</sup>, F. Jung<sup>a\*</sup>

<sup>a</sup> Institute of Biomaterial Science and Berlin-Brandenburg Center for Regenerative Therapies, Helmholtz-Zentrum Geesthacht, Teltow, Germany

<sup>b</sup> Institute of Biotechnology, Brandenburg University of Technology Cottbus-Senftenberg, Senftenberg, Germany

<sup>c</sup> Institute of Chemistry, University of Potsdam, Potsdam, Germany

#: current address: Department of Anesthesia, Pain Management and Perioperative Medicine, Faculty of Medicine, Dalhousie University, Halifax, Canada

\* Corresponding author. E-Mail address: [friedrich.jung@hzg.de](mailto:friedrich.jung@hzg.de)

### **Abstract**

Cyclophosphamide (CPA) is one of the most successful anticancer prodrugs that becomes effective after biotransformation in the liver resulting in the toxic metabolite acrolein. Cancer is often accompanied by thromboembolic events, which might be a result of dysfunctional endothelial cells due to CPA treatment.

Here, the effect of 1 mM CPA or acrolein (10/50/100/500  $\mu$ M) on human umbilical vein endothelial cells (HUVEC) was analyzed after two days of treatment.

The addition of CPA or 10  $\mu$ M acrolein did not affect HUVEC. However, concentrations of 100  $\mu$ M and 500  $\mu$ M acrolein significantly reduced the number of adherent cells by  $86\pm 13\%$

and  $99\pm 1\%$  and cell viability by  $51\pm 29\%$  and  $93\pm 8\%$  compared to the control. Moreover, pronounced stress fibers as well as multiple nuclei were observed and von Willebrand Factor (vWF) was completely released. Lactate dehydrogenase was  $8.5\pm 7.0$ -fold and  $252.9\pm 42.9$ -fold increased showing a loss of cell membrane integrity. The prostacyclin and thromboxane secretion was significantly increased by the addition of  $500\ \mu\text{M}$  acrolein ( $43.1\pm 17.6$ -fold and  $246.4\pm 106.3$ -fold) indicating cell activation/perturbation.

High doses of acrolein led to HUVEC death and loss of vWF production. This effect might be associated with the increased incidence of thromboembolic events in cancer patients treated with high doses of CPA.

**Key words:** human umbilical venous endothelial cells – acrolein – aneuploidy – von Willebrand factor – *in vitro* study

## **Introduction**

Anticancer drugs comprise a large spectrum of agents which mediate their mechanism of action via different routes depending on their target and the application strategy [1]. Whereas some of these drugs are effective *per se*, others only become active after conversion into metabolites produced in the liver (first pass effect). These drugs are called prodrugs. Cyclophosphamide (CPA) is a well-known prodrug with alkylating and antineoplastic activity [2, 3, 4].

After hydroxylation of CPA via cytochrome-P450 oxidases into 4-hydroxy-cyclophosphamide (4-OH-CPA), 4-OH-CPA is able to pass through cellular membranes and thus rapidly enters cells [5, 6]. Within the cell, 4-OH-CPA decomposes to the toxic metabolites; phosphoramidate mustard and acrolein, [5, 6].

CPA is one of the most successful anticancer agents [3]. Two of the resulting metabolites (phosphoramidate mustard and acrolein) have an alkylating effect and are described as toxic to different cell types [3, 7, 8, 9, 10, 11]. In addition, nor-nitrogen mustard – caused by spontaneous decay of CPA - shows an alkylating activity at pH 4.6. However, it is inactive *in vitro* at pH 7.4 and therefore may not have a cytotoxic effect *in vivo* [7, 12].

The maximum dose of CPA clinically used is 60 mg/kg daily administered over two days or 50 mg/kg daily administered over four days. At higher dosages toxic reactions occur [13, 14, 15]. The dose-limiting toxic effect of CPA, observed after administration of high-doses, is cardiotoxicity [4, 16, 17, 18]. CPA can be orally or intravenously administered. During intravenous administration in particular, locally high concentrations in the vasculature can be achieved, possibly inducing damage – not only to cardiomyocytes – but also to endothelial cells (EC), in particular in the infusion area. A first pilot *in vitro* study revealed that the addition of CPA to the cell culture medium (5 or 10 mM, respectively) showed a clear cytostatic effect on human umbilical vein endothelial cells (HUVEC) [19]: HUVEC density decreased in a concentration-dependent manner compared to the untreated control, whereby the viability of adherent HUVEC was not affected. After administration of CPA in cancer patients, cardiac toxicity was described as depending on toxic endothelial damage [15]. Kurauchi *et al.* found acrolein as the main toxic metabolite playing a major role in CPA cardiotoxicity [20].

The average concentration of CPA at 3 hours after administration of high-dose CPA (60 mg/kg) therapy in cancer patients was  $257 \pm 46 \mu\text{M}$  [4]. According to an earlier clinical study this would lead to a concentration of  $3.83 \mu\text{M}$  of phosphoramidate mustard or acrolein [21]. The concentrations of acrolein used in our study were chosen based on results from pharmacokinetic studies of high-dose cyclophosphamide in patients and from other *in vitro* studies [4, 20] between 10 and  $500 \mu\text{M}$ . In addition, it is known that not only hepatocytes but also endothelial cells endogenously express cytochrome P450 enzymes, which theoretically

enable them to convert CPA into acrolein. Thus, local acrolein concentrations in endothelial cells could be higher than in their environment (serum or urine) where they are typically measured. Since metabolites of CPA were shown to be present at low levels after 50 hours after intravenous injection [22], an exposure time of 2 days was chosen.

A recent study corroborated the cytotoxic potency of acrolein and described acrolein to be the main toxic metabolite for cardiomyocytes [4]. Therefore, in the study presented here, the effect of acrolein on endothelial cells in comparison to CPA was evaluated.

## **Material and Methods**

### *Cultivation and treatment of HUVEC*

Human umbilical vein endothelial cells (HUVEC, Lonza, Cologne, Germany) were cultivated in endothelial cell culture medium supplemented with 5% (v/v) fetal bovine serum (Upcyte technologies GmbH, Hamburg, Germany). Cells were used at passage 4 for experiments [23]. HUVEC were seeded on glass coverslips (Th. Geyer GmbH, Hamburg, Germany) in 24-well plates (TPP, Techno Plastic Products AG, Trasadingen, Switzerland) with a cell density of 20,000 cells/well to keep cells in growing phase throughout the experimental setup. After 24 h, the cell culture medium was replaced by fresh medium containing 1 mM CPA (Alfa Aesar, Kandel, Germany, CAS-number: 6055-19-2, >97% purity) or acrolein in concentrations of 10  $\mu$ M, 50  $\mu$ M, 100  $\mu$ M or 500  $\mu$ M (Sigma-Aldrich, Taufkirchen, Germany, CAS-number: 107-02-8, analytical standard grade). The structural formulas of CPA and acrolein are shown in figure 1. As a (negative) control, cells were cultivated in pure cell culture medium. Analyses regarding cell viability, expression of von Willebrand factor and actin filaments, cell membrane integrity and secretion of prostacyclin were performed after 2 d of treatment. The study design is presented in Figure 2.



### *Cell Viability*

The analysis of the cell viability was performed using fluorescein diacetate (FDA,  $12.5 \mu\text{g}\cdot\text{mL}^{-1}$ , Invitrogen, Carlsbad, CA, USA) to stain vital cells in green and propidium iodide (PI,  $1 \mu\text{g}\cdot\text{mL}^{-1}$ , Sigma-Aldrich, Taufkirchen, Germany) to stain dead cells in red. For this, FDA and PI were added to the cell culture medium and images of HUVEC were immediately taken in a 20-fold magnification (Laser scanning microscope Axiovert 200M, Zeiss, Oberkochen, Germany). The number of live and dead cells were counted using ImageJ (U. S. National Institutes of Health, Bethesda, Maryland, USA, <https://imagej.nih.gov/ij/>) and expressed as a percentage of the total cell number. The number of vital adherent cells was calculated relative to the growth area in  $\text{mm}^2$ .

### *Fluorescence staining*

To assess the cell morphology, cells were stained with phalloidin to visualize actin filaments and antibodies to detect von Willebrand factor. Briefly, cells were fixed with 4% (w/v) paraformaldehyde (Sigma-Aldrich, Taufkirchen, Germany) for 30 min, permeabilized using 0.5% (v/v) Triton-X-100 for 10 min (Sigma-Aldrich, Taufkirchen, Germany) and unspecific binding sites were blocked with 5% (w/v) bovine serum albumin (Roth, Karlsruhe, Germany) for 20 min at room temperature. Phalloidin conjugated to Alexa Fluor 555 (Invitrogen, Carlsbad, CA, USA, 1:40) and the primary rabbit anti-human von Willebrand factor-directed antibody (Sigma-Aldrich, Taufkirchen, Germany, F3520, 1:200) were incubated for 1 h at room temperature in the dark. After three washing steps with phosphate buffered saline (Invitrogen, Carlsbad, CA, USA) cells were incubated with the secondary donkey anti-rabbit antibody conjugated to Alexa Fluor 488 (Invitrogen, Carlsbad, CA, USA, A21206, 1:400) for 1 h at room temperature in the dark. Finally, cells were washed again and covered with

mounting medium containing 4',6-diamidino-2-phenylindole (Roth, Karlsruhe, Germany) to counterstain cell nuclei in blue.

#### *Measurement of cell membrane integrity*

Cell membrane integrity was measured using the LDH Cytotoxicity Assay Kit II (LDH, Roche, Grenzach, Germany) according to the manufacturer's instructions. Briefly, cells were seeded in 96-well plates (Greiner Bio One, Leipzig, Germany) with 5,000 cells/well and treated with CPA and acrolein as described above. Three days after seeding, 10  $\mu$ L of cell culture supernatant was added to 100  $\mu$ L of LDH reaction mix. After 30 min incubation at room temperature in the dark, the absorbance at 450 nm (reference wavelength: 650 nm) was measured using a photometer (Tecan infinite M200 pro, Crailsheim, Germany) and the LDH release was normalized to the number of adherent cells.

#### *Quantification of prostacyclin and thromboxane B2*

Prostacyclin and thromboxane B2 secretion was quantified using a competitive enzyme immunoassay (6-keto Prostaglandin F<sub>1 $\alpha$</sub>  ELISA Kit and Thromboxane B2 ELISA Kit, Cayman Chemical, Hamburg, Germany) according to the manufacturer's instructions. Briefly, 50  $\mu$ L cell culture supernatant were used per well and measurements were performed in triplicates. Absorbance was recorded at 410 nm using a photometer (Tecan infinite M200 pro, Crailsheim, Germany). Prostacyclin and thromboxane B2 concentrations were calculated based on a standard curve and normalized to the number of adherent cells per well.

### *Statistics and error consideration*

Statistical analyses were performed using Graphpad Prism 6 (Graphpad Software, San Diego, California). Normal distribution of the data was tested using the d'Agostino & Pearson omnibus normality test. Data are reported as arithmetic mean  $\pm$  standard deviation for continuous variables. Multiple comparisons between groups were performed by two-way ANOVA and Dunnett's *post hoc* test for normally distributed data and Kruskal-Wallis test with Dunn's *post hoc* test for non-parametric data. Differences were considered significant at  $p < 0.05$ .

## **Results**

### *Density of adherent HUVEC*

Figure 3 shows HUVEC densities as cell numbers/mm<sup>2</sup> at the third day after seeding. The seeding experiments up to three days confirmed that HUVEC were able to adhere and proliferate to confluence on glass coverslips in tissue culture plates.

Supplementation of the cell culture medium with 1 mM CPA or with 10  $\mu$ M acrolein had no influence on the number of adherent HUVEC. However, already at an acrolein concentration of 50  $\mu$ M, the number of adherent HUVEC decreased by 26 $\pm$ 50% according to tendency. Treatment with 100  $\mu$ M and 500  $\mu$ M acrolein reduced the number of adherent cells significantly by 86 $\pm$ 13% (100  $\mu$ M,  $p < 0.0001$ ) and 99 $\pm$ 1% (500  $\mu$ M,  $p = 0.0003$ ) compared to the control (Fig. 3).

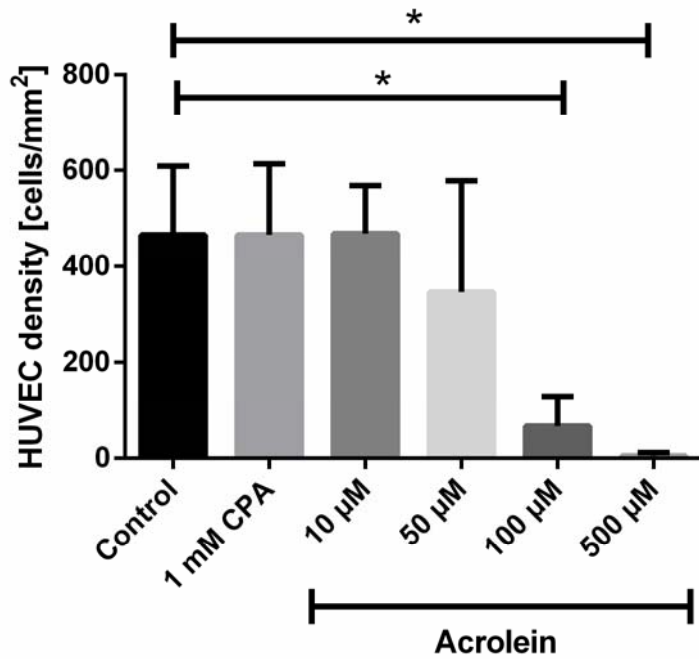


**Figure 3:** Human umbilical vein endothelial cells (HUVEC) densities [cells/mm<sup>2</sup>] at the third day after seeding. HUVEC were cultivated for one day before they were treated with cyclophosphamide (1 mM CPA) or acrolein (10 µM, 50 µM, 100 µM or 500 µM) for two days. Control cells were cultivated with pure cell culture medium (arithmetic mean ± standard deviation; n=6).

#### *Viability of adherent HUVEC*

Representative images of HUVEC monolayers are shown in figure 4 (phase microscopy - upper row; live/dead staining - lower row). Both phase contrast images and live/dead staining show that cells treated with 1 mM CPA and 10 µM acrolein look similar to control cells. Treatment with 50 µM acrolein induced some cell detachment and few dead cells. Dramatic changes in cell viability were observed after adding 100 µM and 500 µM acrolein. Under these conditions most of the cells detached from the substrate and remained as round and dying cells in the cell culture medium. Quantification of the number of viable and dead cells showed that

with increasing acrolein concentration not only the number of adherent HUVEC decreased, but also the number of dead adherent HUVEC.

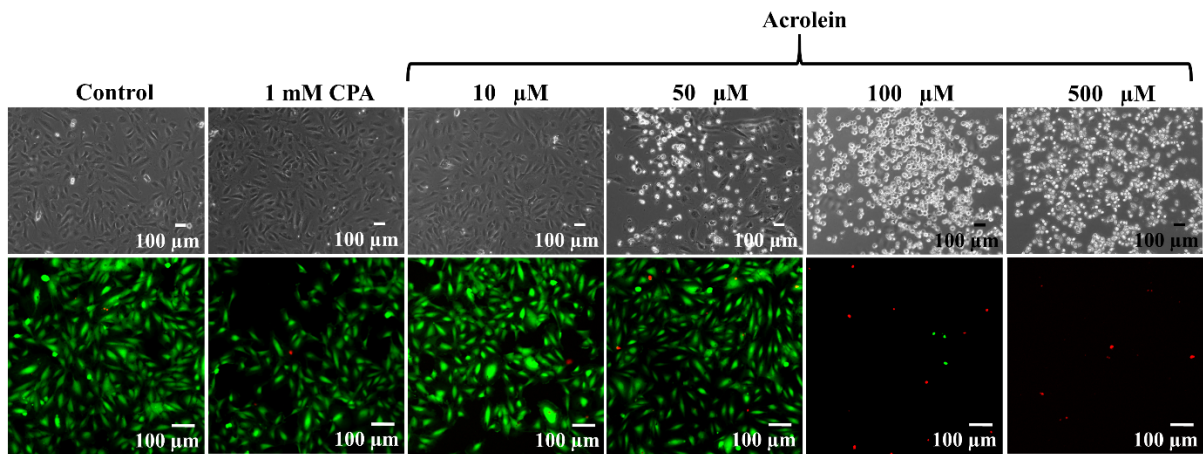


**Figure 4:** Representative images of the human umbilical vein endothelial cell (HUVEC) monolayers after adding cyclophosphamide (CPA) or acrolein. After one day of cultivation, HUVEC were treated with CPA or increasing amounts of acrolein. Control cells were cultivated in pure cell culture medium. Upper row: phase contrast microscopy (10-fold magnification); lower row: live (green)/dead (red) staining imaged by confocal laser scanning microscopy (20-fold magnification).

Figure 5 shows that at an acrolein concentration of 50  $\mu\text{M}$   $5\pm 13\%$  of the adherent HUVEC were dead, at 100  $\mu\text{M}$  nearly half of the adherent HUVEC were dead ( $p < 0.0001$ ) and at the concentration of 500  $\mu\text{M}$  already  $93\pm 8\%$  ( $p < 0.0001$ ) of the adherent HUVEC were dead.

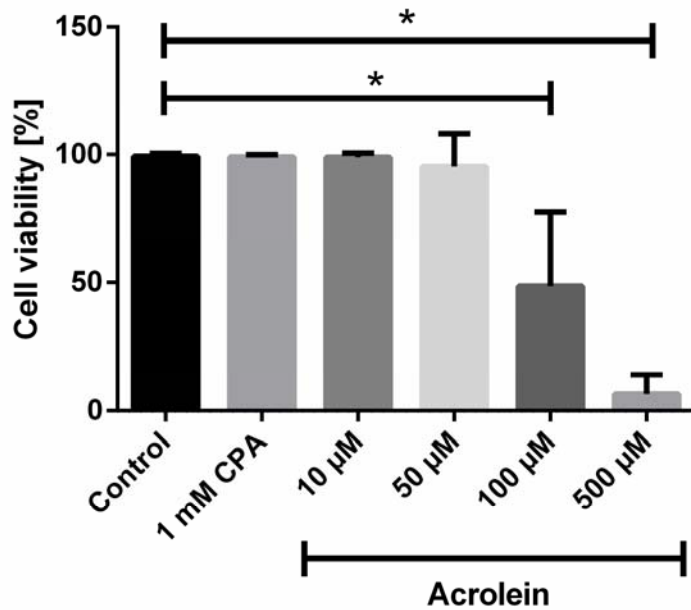


**Figure 5:** Viable adherent human umbilical vein endothelial cells (HUVEC) in [%] at the third day after seeding. After one day of cultivation, HUVEC were treated with cyclophosphamide (1 mM) or acrolein (10 µM, 50 µM, 100 µM or 500 µM) for two days. Control cells were cultivated in pure cell culture medium (arithmetic mean  $\pm$  standard deviation; n=6).

#### *Morphology of the adherent HUVEC*

After three days of seeding, most untreated HUVEC exhibited a large, spindle-shape and were randomly organized. Confluence was not yet reached. However, HUVEC started to decrease their stress fibers in central parts of the cells and there was a tendency of marginal filament band broadening. Most adherent cells contained von Willebrand factor, so that the cells could be unambiguously characterized as endothelial cells (Fig. S1).

After adding 1 mM CPA or 10 µM acrolein slightly more stress fibers were found compared to the control cells (data not shown).

The addition of 50  $\mu\text{M}$  acrolein to the cell culture medium revealed a disturbance of the microfilament structure. A disconnection of cell-cell contacts and the appearance of minute intercellular fenestrations was visible.

Dramatic changes occurred after adding 100  $\mu\text{M}$  acrolein to the culture medium. Far fewer, and smaller HUVEC, with completely changed morphology adhered and more than half of the adherent cells showed an increased number of nuclei. In contrast to the control, stress fibers in central parts of the cells were not located towards the outer rim of the cells indicating no development of a functionally-confluent monolayer. In addition, vWF could not be detected in HUVEC anymore. Treatment with 500  $\mu\text{M}$  acrolein led to few cellular fragments or shrunken HUVEC containing a high number of nuclei. Also, here, no vWF was visible (Fig. 6).

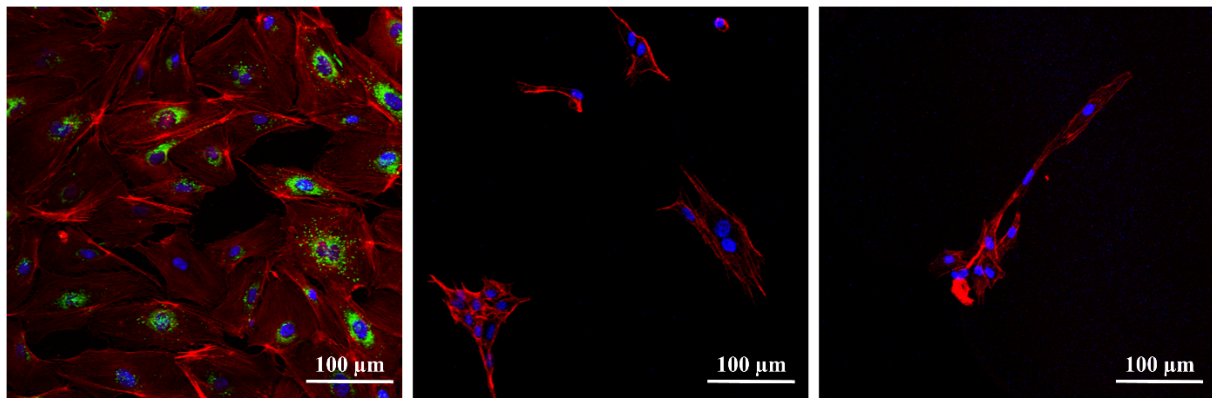


**Figure 6:** Actin and von Willebrand (vWF) expression in adherent human umbilical vein endothelial cells (HUVEC) treated with acrolein (50  $\mu\text{M}$ -left, 100  $\mu\text{M}$ -mid, 500  $\mu\text{M}$ -right) for two days. Actin is stained in red, vWF in green, nuclei in blue. Images were acquired by confocal laser scanning microscopy (20-fold magnification).

#### *Investigation of the integrity of the membrane of adherent HUVEC*

CPA or acrolein in concentrations between 10  $\mu\text{M}$  to 50  $\mu\text{M}$  did not affect the concentration of lactate dehydrogenase (LDH) in the HUVECs' cell culture medium of compared to controls

after two days of treatment (Fig. 7). However, treatment with 100  $\mu\text{M}$  acrolein significantly increased the amount of free LDH in the supernatant ( $8.5\pm 7.0$ -fold,  $p=0.0023$ ). At the highest concentration of acrolein of 500  $\mu\text{M}$  the increase of LDH was even more pronounced ( $252.9\pm 42.9$ -fold,  $p<0.0001$ ).

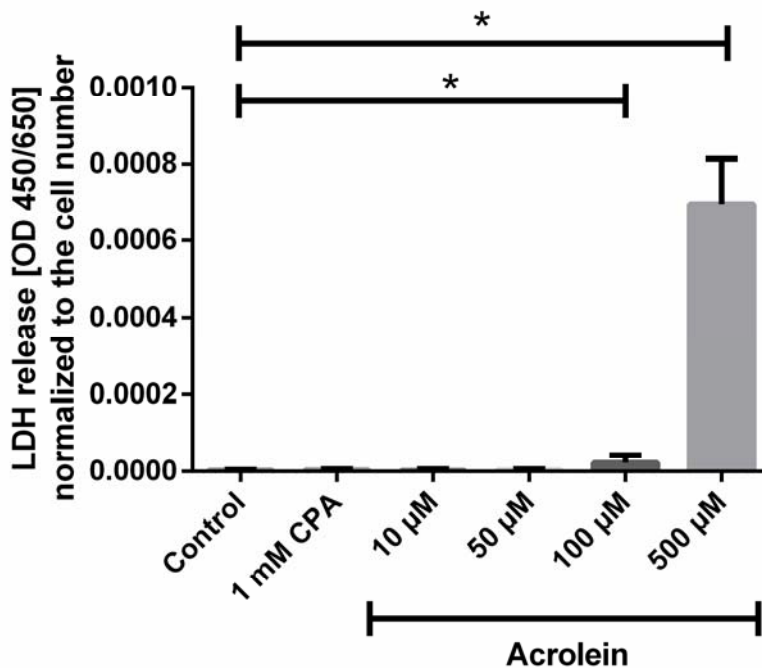


**Figure 7:** Integrity of the membrane of adherent human umbilical vein endothelial cells (HUVEC) normalized to the cell number per well at the third day after seeding. After one day of cultivation, HUVEC were treated with 1 mM cyclophosphamide (CPA) or increasing concentrations of acrolein (10  $\mu\text{M}$ , 50  $\mu\text{M}$ , 100  $\mu\text{M}$  or 500  $\mu\text{M}$ ) for two days. Control cells were cultivated in pure cell culture medium (arithmetic mean  $\pm$  standard deviation;  $n=6$ ).

*Prostacyclin and thromboxane B2 production of adherent HUVEC*

The addition of 1 mM CPA and acrolein in concentrations of 10  $\mu$ M to 100  $\mu$ M had no significant effect on the prostacyclin secretion by adherent HUVEC. A slight increase ( $1.7\pm 1.1$ -fold and  $6.7\pm 2.5$ -fold) in the prostacyclin secretion was evident after treatment with 50  $\mu$ M and 100  $\mu$ M of acrolein, however, this increase was not statistically relevant. In contrast, treatment with 500  $\mu$ M acrolein induced a  $43.1\pm 17.6$ -fold increase in the prostacyclin concentration ( $p < 0.0001$ ; Fig. 8).

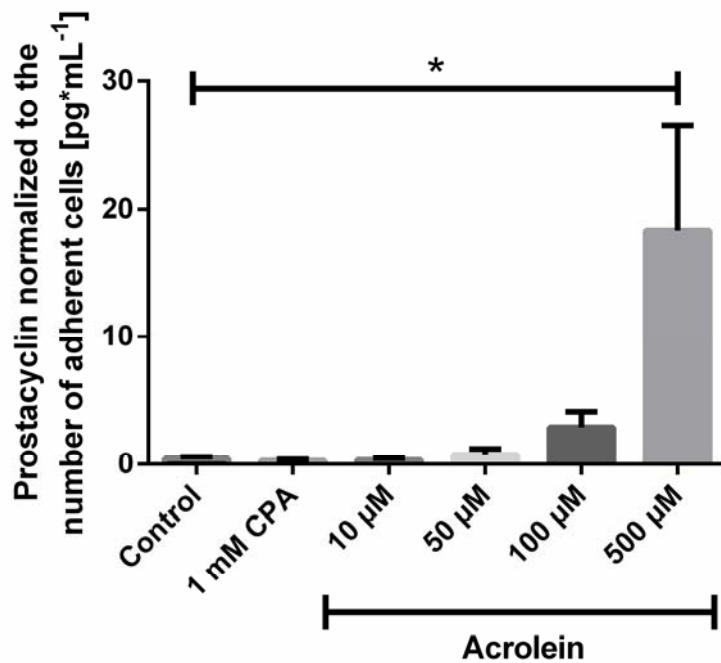


**Figure 8:** Prostacyclin secretion normalized to the number of adherent human umbilical vein endothelial cells (HUVEC). HUVEC were cultivated for one day before they were treated with 1 mM cyclophosphamide (CPA) or acrolein (10  $\mu$ M, 50  $\mu$ M, 100  $\mu$ M or 500  $\mu$ M) for two days. Control cells were cultivated with pure cell culture medium (arithmetic mean  $\pm$  standard deviation;  $n=6$ ).

A similar effect of CPA and acrolein was observed regarding the secretion of thromboxane B<sub>2</sub>. CPA and acrolein in concentrations of 10  $\mu$ M to 50  $\mu$ M had no significant effect on the

thromboxane B2 secretion. Addition of 100  $\mu\text{M}$  acrolein slightly increased the concentration of thromboxane B2 in the supernatant ( $8.0\pm 3.1$ -fold) but not in a statistically relevant manner. However, treatment with 500  $\mu\text{M}$  acrolein induced a  $246.4\pm 106.3$ -fold increase in the secretion of thromboxane B2 ( $p=0.0347$ ; Fig. 9).

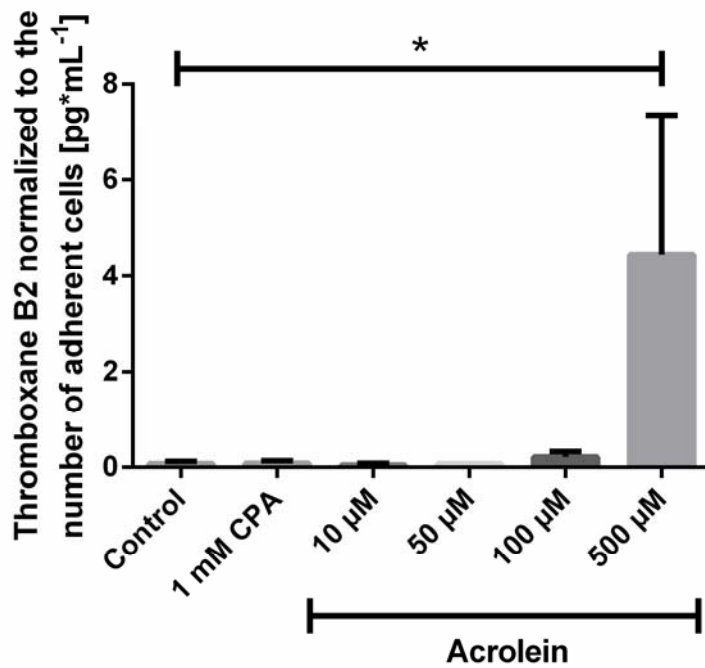


**Figure 9:** Thromboxane B2 secretion normalized to the number of adherent human umbilical vein endothelial cells (HUVEC). HUVEC were cultivated for one day before they were treated with 1 mM cyclophosphamide (CPA) or acrolein (10  $\mu\text{M}$ , 50  $\mu\text{M}$ , 100  $\mu\text{M}$  or 500  $\mu\text{M}$ ) for two days. Control cells were cultivated with pure cell culture medium (arithmetic mean  $\pm$  standard deviation;  $n=6$  for control and CPA,  $n=5$  for 10  $\mu\text{M}$  and 100  $\mu\text{M}$  acrolein,  $n=3$  for 500  $\mu\text{M}$  acrolein and  $n=1$  for 50  $\mu\text{M}$  acrolein).

## Discussion

The study revealed a toxic effect of acrolein on endothelial cells in a dose-dependent manner. With increasing acrolein concentration (between 10  $\mu\text{M}$  up to 500  $\mu\text{M}$ ) the number of adherent HUVEC decreased significantly. At the highest acrolein concentration (500  $\mu\text{M}$ ) only  $5\pm 7$  HUVEC/ $\text{mm}^2$  adhered (compared to  $466\pm 143$  in the control cultures). It has been shown that acrolein induces cell death via apoptosis or necrosis depending on the cell type. Human lung macrophages [24] and lung epithelial cells [25] as well as human keratinocytes [26] undergo apoptosis whereas murine proB lymphoid progenitor cells [27] become necrotic in response to acrolein. A study by Misonou *et al.* suggested that HUVEC exposed to acrolein underwent cell death via apoptotic pathways as shown by staining of highly condensed DNA as a marker for apoptosis [28]. However, markers for necrosis were not investigated in this study. Tanel and Averill-Bates demonstrated a concentration-dependent effect of acrolein on the mechanism of cell death [29]. At lower concentrations (up to 50 fmol/cell) cells underwent apoptosis. At higher concentrations (100 fmol/cell) necrosis was induced e.g. in chinese hamster ovary cells. From a mechanistic point of view, acrolein-induced apoptosis was mediated through the mitochondrial pathway involving the release of cytochrome c from mitochondria and the activation of caspases [29]. In addition, apoptosis can also be initiated by the endoplasmic reticulum as shown in lung epithelial cells [25]. However, alternative or complementary mechanisms might also contribute to acrolein-mediated apoptosis. Regardless of the underlying molecular mechanism, these studies demonstrated that the presence of acrolein led to cell death, which is well in line with our findings. Initial morphological responses were found at a concentration of 50  $\mu\text{M}$  acrolein. At this concentration  $5\pm 13\%$  of HUVEC were dead, at 100  $\mu\text{M}$  more than half of cells and at a concentration of 500  $\mu\text{M}$  nearly all ( $93\pm 8\%$ ) HUVEC. In addition, particularly pronounced stress fibers in central parts of the HUVEC were found and the amount of vWF in the cells started to decrease. Particularly noticeable was the

absence of vWF at concentrations of 100  $\mu\text{M}$  or 500  $\mu\text{M}$  acrolein. vWF is synthesized in endothelial cells and stored in specific cell organelles, the Weibel Palade bodies (WPBs), as can be seen in the control HUVEC or in cultures supplemented with the low dosage of acrolein. From there it can be released by exocytosis after stimulation by different mediators and after cell damage to support platelet adhesion and subsequent thrombus formation [30]. A deficiency of vWF, however, is associated with severe bleeding disorders. Thus, the complete absence of vWF in cells treated with the two highest doses of acrolein indicates a dramatic damage of the cellular function.

Also, the shape of the HUVEC changed dramatically; at 500  $\mu\text{M}$  only very few fragments or shrunken HUVEC were visible. At the same time almost only aneuploid cells were recognizable with some cells containing up to 6 nuclei (see Fig. 6). It has been shown by Bahl *et al.* [31] that 24 hours of treatment with acrolein decreased the expression of transcription factor Dp-1, a factor needed for the G1 to S transition in the cell cycle [32]. Obviously, duplication of DNA and nuclei take place but not cell division. The significance of multiple nuclei remains still obscure. In the present case, it can be interpreted as pathological condition [33].

The LDH concentration, which is significantly elevated in the supernatant after treatment with 100  $\mu\text{M}$  or 500  $\mu\text{M}$  acrolein, shows that the integrity of the cell membrane is no longer intact. This is a reflection of the cell viability (Fig. 5), which was significantly reduced at these concentrations. Cell death is accompanied by decreased membrane integrity leading to the secretion of intracellular fluids involving LDH. The cell membrane damaging effect of acrolein was shown for a number of other cells types, however, with varying sensitivities to acrolein. Whereas murine pro B lymphoid progenitor cells showed a significant LDH release in response to 20  $\mu\text{M}$  acrolein for 30 min [27], porcine pulmonary artery endothelial cells secreted a significant amount of LDH after treatment with 4.5  $\mu\text{M}$  acrolein for 30 min [34]. In the present

study, HUVEC released LDH in a statistically relevant amount after stimulation with extremely high concentrations of 100  $\mu$ M and 500  $\mu$ M acrolein for 48 hours. This indicates that HUVEC are much more resistant to acrolein than murine hemopoietic cells or porcine endothelial cells.

Prostacyclin (PGI<sub>2</sub>) was quantified in the HUVEC supernatant to assess the activation state of the HUVEC. Physiologically, endothelial cells show an anti-thrombotic phenotype characterized by the hydrolyzation of adenosine triphosphate (ATP) and adenosine diphosphate (ADP) preventing platelet activation, adhesion and aggregation by expressing 13-hydroxyoctadecadienoic acid and releasing prostacyclin among other molecules [35]. Endothelial cells respond to changes in their environment within minutes [36]. This acute response follows receptor-mediated cell signaling accompanied by influx of calcium ions and induction of various types of phosphorylations which result in i.) the activation of enzymes that generate PGI<sub>2</sub>, and ii.) the recruitment of vesicles with pre-formed proteins to the plasma membrane reinforcing endothelial cell activation [37]. The increase of released prostacyclin indicates a state described as perturbation of endothelial cells [38-42]. In this study, treatment of HUVEC with 100  $\mu$ M and 500  $\mu$ M acrolein increased the PGI<sub>2</sub> secretion 6.7 $\pm$ 2.5-fold and 43.1 $\pm$ 17.6-fold, respectively, compared to the control. These findings clearly show that the HUVEC were in a highly activated or perturbed state depending on the acrolein concentration: with increasing acrolein concentration, PGI<sub>2</sub> increased exponentially which underlines the toxic effect of high doses of acrolein. Moreover, the secretion of thromboxane B<sub>2</sub> was 246.4 $\pm$ 106.3-fold increased after treatment with 500  $\mu$ M acrolein compared to the control. Thromboxane B<sub>2</sub> is a more stable metabolite of thromboxane A<sub>2</sub>, which is released by endothelial cells at events of tissue injury and inflammation [43]. Thromboxane A<sub>2</sub> induces platelet activation and aggregation *in vitro* as well as *in vivo* [44]. In addition, it acts as a potent vasoconstrictor resulting in narrowed vessel diameters reducing the blood flow. The platelet activating potency of thromboxane is four orders of magnitude higher than the inhibiting

potency of prostacyclin [44] leading to a very high risk of platelet activation and aggregation in an *in vivo* setting. Thus, the increased release of thromboxane after treatment with 500  $\mu\text{M}$  acrolein indicates that HUVEC were exposed to a severe pathological setting and thus reacted with pro-thrombotic actions.

### *Clinical Impact*

The perturbation/activation of the endothelium accompanied by the acrolein-induced dosage-dependent detachment and death of adherent endothelial cells would *in vivo* lead to the formation of intercellular gaps and subsequently to the formation of denuded subendothelial matrix areas triggering thrombocyte adherence and thrombus growth [45-47].

The thrombogenicity of acrolein is amplified by the release of von Willebrand factor, especially at very high dosages. Weibel-Palade bodies (WPBs) harbor multiple pro-inflammatory and pro-hemostatic proteins [48], including the leukocyte receptor P-selectin, the pro-hemostatic glycoprotein von Willebrand factor (vWF), pro-inflammatory cytokines, and agents that control tonicity [49]. Within minutes of secretagogue stimulation, WPBs undergo exocytosis [48], releasing their content into the blood, which initiates hemostasis. On denuded vascular wall areas, the interaction between the membrane receptor GPIIb/IIIa with the subendothelial-bound vWF will initiate the tethering of circulating platelets to the vessel wall. Tethering platelets to vWF is rapidly followed by platelet binding to collagen through specific receptors (GPVI and  $\alpha_2\beta_1$ ) leading to firm adhesion, activation, and additional stable bonds mediated by the  $\alpha\text{IIb}\beta_3$  integrin complex [50, 51]. Upon exocytosis, the tubules unfurl into long protein strings, which recruit neighbored platelets even at non-pathological shear [52] leading from initially bound singular platelets to thrombus formation - interactions that can result in pathological thrombosis formation.

Furthermore, vWF carries coagulation factor VIII, which is involved in thrombin formation that, in addition to activating platelets, mediates – beneath several other actions - fibrin formation and thus the stabilization of the growing thrombus [53].

This pro-thrombotic scenario is further reinforced by the release of thromboxane, a strong stimulator of platelet activation [54], which dramatically increases at very high doses of acrolein.

The results of the *in vitro* study presented here coincide well with clinical findings. On the basis of postmortem examinations, the pathophysiology of high-dose CPA-associated cardiac toxicity is thought to depend on toxic endothelial damage [19] followed by extravasation of toxic metabolites, resulting in myocyte damage, interstitial hemorrhage, and edema [15, 18].

In addition, approximately 15% of cancer patients suffer from thromboembolic events, in patients with bronchial carcinoma up to 28% [55, 56]. The exact cause is mostly unknown. In fact, the percentage of thromboembolic events in cancer patients is significantly higher; postmortem examinations in 1505 autopsies with malignant disease showed either venous thrombosis, pulmonary embolism, or both (40.3%) in 607 of the included patients [56].

It can be hypothesized that possibly a certain percentage of the thrombotic events might be caused by the antineoplastic agents.

### *Conclusion*

The study revealed that acrolein led to an activation, to the detachment and death of endothelial cells and at high or very high dosages to aneuploidy and the complete loss of von Willebrand factor. This would *in vivo* lead to denuded, subendothelial areas and together with the release of von Willebrand factor and thromboxane to a situation with a high risk for thrombotic events.

## **Acknowledgments**

The work was financially supported by the Helmholtz-Association through programme-oriented funding; by the European Regional Development Funds (EFRE, Brandenburg, Germany) through the project “PERsonalisierte Medizin durch FUNCTIONomics in Berlin-Brandenburg”; and by the Ministry for Science, Research and Cultural Affairs of Brandenburg through the grant of the joint project “Konsequenzen der altersassoziierten Zell- und Organfunktionen” of the Gesundheitscampus Brandenburg; and through the project “Endothelfunktionstestung mit Medikamenten und isolierten Metaboliten” (project number: 85002925).

## **References**

- [1] Olgen S. Overview on Anticancer Drug Design and Development. *Curr Med Chem.* 2018;25(15):1704-1719.
- [2] Chang THK, Weber GF, Crespi CL, Waxman DJ. Differential Activation of Cyclophosphamide and Ifosfamide by Cytochromes P-450 2B and 3A in Human Liver Microsomes. *Cancer Research.* 1993;53:5629-5637.
- [3] Emadi A, Jones RJ, Brodsky RA. Cyclophosphamide and cancer: golden anniversary. *Nat Rev Clin Oncol.* 2009;6(11):638-47.
- [4] Nishikawa T, Miyahara E, Kurauchi K, Watanabe E, Ikawa K, Asaba K, Tanabe T, Okamoto Y, Kawano Y. Mechanisms of Fatal Cardiotoxicity following High-Dose Cyclophosphamide Therapy and a Method for Its Prevention. *Plos One.* 2015;10(6):e0131394.

- [5] Huitema A, Tibben M, Kerbusch T, Kettenes-van den Bosch JJ, Rodenhuis S, Beijnen JH. High performance liquid chromatographic determination of the stabilized cyclophosphamide metabolite 4-hydroxycyclophosphamide in plasma and red blood cells. *J Liq Chrom Rel Technol.* 2000;23:1725–1744.
- [6] Ren S, Kalhorn T, McDonald GB, Anasetti C, Appelbaum FR, Slattery JT. Pharmacokinetics of cyclophosphamide and its metabolites in bone marrow transplantation patients. *Clin Pharmacol Ther.* 1998;64:289–301.
- [7] Colvin M, Brundrett RB, Kan MN, Jardine I, Fenselau C: Alkylating properties of phosphoramidate mustard. *Cancer Res.* 1976;36:1121-1126.
- [8] Clarke L, Waxman, DJ. Oxidative metabolism of cyclophosphamide: identification of the hepatic monooxygenase catalyts of drug activation. *Cancer Res.* 1989;49:2344-2350.
- [9] Giraud B, Herbert G, Deroussent A, Veal GJ, Vassal G, Paci A. Oxazaphosphorines: new therapeutic strategies for an old class of drugs. *Expert Opin Drug Metab Toxicol.* 2010;6(8):919-38.
- [10] Huong CH, Chen YT, Lin JH, Wang HT. Acrolein induces ribotoxic stress in human cancer cells regardless of p53 status. *Toxicol in vitro.* 2018;52:265-271.
- [11] Luo S, Jiang L, Li Q, Sun X, Liu T, Pei F, Zhang T, Liu T, Dong L, Liu X, Jiang L. Acrolein-induced autophagy-dependent apoptosis via activation of the lysosomal-mitochondrial pathway in EAhy926 cells. *Toxicol in vitro.* 2018;52:146-153.

- [12] Juma FD, Rogers HI, Trounc JR. The pharmacocinetics of cyclophosphamide, phosphoramidate mustard and NOR-nitrogen mustard studied by gas chromatography in patients receiving cyclophosphamide Therapy. *Br J clin Pharmacol.* 1980;10:327-335.
- [13] Santos GW, Sensenbrenner LL, Burke PJ, Mullins GM, Blas WB, Tutschka PJ, Slavin RE. The use of cyclophosphamide for clinical marrow transplantation. *Transplant Proc.* 1972;4:559–564.
- [14] Murdych T, Weisdorf DJ. Serious cardiac complications during bone marrow transplantation at the University of Minnesota,1977–1997. *Bone Marrow Transplant.* 2001;28:283–287.
- [15] Cazin B, Gorin NC, Laporte JP, Gallet B, Douay L, Lopez M, Najman A, Duhamel G. Cardiac complications after marrow transplantation. A report on a series of 63 consecutive transplantation. *Cancer.* 1986;57:2061.
- [16] Ayash LJ, Wright JE, Tretyakov O, Gonin R, Elias A, Wheeler C,Eder JP, Rosowsky A, Antman K, Frei E 3rd. Cyclophosphamide pharmacokinetics: correlation with cardiotoxicity and tumor response. *J Clin Oncol.* 1992;10:995–1000.
- [17] Braverman AC, Antin JH, Plappert MT, Cook EF, Lee RT. Cyclophosphamide cardiotoxicity in bone marrow transplantation: a prospective evaluation of new dosing regimens. *J Clin Oncol.* 1991;9:1215– 1223.
- [18] Mills BA, Roberts RW. Cyclophosphamide-induced cardiomyopathy: a report of two cases and review of the English literature. *Cancer.* 1979;43:2223–2226.

- [19] Krüger-Genge A, Steinbrecht S, Küpper JH, Lendlein A, Jung F. Evidence for cytostatic effect of cyclophosphamide on human vein endothelial cells in cancer therapy: Preliminary in vitro results. *Clin Hemorheol Microcirc.* 2018;69:267–276.
- [20] Kurauchi K, Nishikawa T, Miyahara E, Okamoto Y, Kawano Y. Role of metabolites of cyclophosphamide in cardiotoxicity. *BMC Res Notes.* 2017;10:406.
- [21] Struck RF, Alberts DS, Horne K, Phillips JG, Peng Y-M, Roe DJ. Plasma Pharmacokinetics of Cyclophosphamide and Its Cytotoxic Metabolites after Intravenous versus Oral Administration in a Randomized, Crossover Trial. *Cancer Research.* 1987;47:2723-2726.
- [22] Kalhorn T. F, Ren S, Howald W. N, Lawrence R. F, Slattery J. T. Analysis of cyclophosphamide and five metabolites from human plasma using liquid chromatography–mass spectrometry and gas chromatography–nitrogen–phosphorus detection. *J Chromatogr Biomed Sci Appl.* 1999; 732(2):287-98.
- [23] Krüger A, Fuhrmann R, Jung F, Franke RP. Influence of the coating with extracellular matrix and the number of cell passages on the endothelialization of a polystyrene surface. *Clin Hemorheol Microcirc.* 2015;60:153–161.
- [24] Li L, Hamilton RF Jr, Taylor DE, Holian A, Acrolein-induced cell death in human alveolar macrophages. *Toxicol Appl Pharmacol.* 1997;145(2):331-9.
- [25] Tanel A, Palapati P, Bettaieb A, Morin P, Averill-Bates DA. Acrolein activates cell survival and apoptotic death responses involving the endoplasmic reticulum in A549 lung cells. *Biochim Biophys Acta.* 2014;1843(5):827-35.

- [26] Takeuchi, K., Kato, M., Suzuki, H., Akhand, A. A., Wu, J., Hossain, K., Miyata, T., Matsumoto, Y., Nimura, Y., Nakashima, I. Acrolein induces activation of the epidermal growth factor receptor of human keratinocytes for cell death. *J Cell Biochem.* 2001;81(4):679-88.
- [27] Kern JC, Kehrer JP. Acrolein-induced cell death: a caspase-influenced decision between apoptosis and oncosis/necrosis. *Chem Biol Interact.* 2002;139(1):79-95.
- [28] Misonou Y, Asahi M, Yokoe S, Miyoshi E, Taniguchi N. Acrolein produces nitric oxide through the elevation of intracellular calcium levels to induce apoptosis in human umbilical vein endothelial cells: implications for smoke angiopathy. *Nitric Oxide.* 2006;14(2):180-7.
- [29] Tanel A, Averill-Bates DA. The aldehyde Acrolein induces apoptosis via activation of the mitochondrial pathway. *Biochim Biophys Acta.* 2005;1743(3):255-67.
- [30] Lowenstein CJ, Morrell CN, Yamakuchi M. Regulation of Weibel-Palade body exocytosis. *Trends Cardiovasc Med.* 2005;15(8):302-8.
- [31] Bahl V, Weng NJ, Schick SF, Sleiman M, Whitehead J, Ibarra A, Talbot P. Cytotoxicity of Thirdhand Smoke and Identification of Acrolein as a Volatile Thirdhand Smoke Chemical That Inhibits Cell Proliferation. *Toxicol Sci.* 2016;150(1):234-46.
- [32] Nightingale TD, McCormack JJ, Grimes W, Robinson C, Lopes da Silva M, White IJ, Vaughan A, Cramer LP, Cutler DF. Tuning the endothelial response: differential release of exocytic cargos from Weibel-Palade bodies. *J Thromb Haemost.* 2018;16(9):1873-1886.
- [33] Dahl E. The fine structure of nuclear inclusions. *J Anat.* 1970;106:255–262.

- [34] Patel JM, Block ER. Acrolein-induced injury to cultured pulmonary artery endothelial cells. *Toxicol Appl Pharmacol*. 1993;122(1):46-53.
- [35] Michiels C. Endothelial cells functions. *J Cell Physiol*. 2003;193:430-43.
- [36] Franke R-P, Fuhrmann R, Hiebl B, Jung F. Influence of various radiographic contrast media on the buckling of endothelial cells. *Microvasc Res*. 2008;76:110-3.
- [37] van Hinsbergh VWM. Endothelium—role in regulation of coagulation and inflammation. *Semin Immunopathol*. 2012;34:93-106.
- [38] Brox JH, Nordøy A. Prostacyclin and <sup>51</sup>Cr release in cultured human endothelial cells. *Pathophysiol of Haemostasis Thromb*. 1982;12:345-52.
- [39] Hauser S, Jung F, Pietzsch J. Human Endothelial Cell Models in Biomaterial Research. *Trends Biotechnol*. 2017;35(3):265-277.
- [40] Holland J, Pritchard K, Rogers N, Stemerman M. Perturbation of cultured human endothelial cells by atherogenic levels of low density lipoprotein. *Am J Pathol*. 1988;132:474.
- [41] Krüger-Genge A, Schulz C, Kratz K, Lendlein A, Jung F. Comparison of two substrate materials used as negative control in endothelialization studies: Glass versus polymeric tissue culture plate. *Clin Hemorheol Microcirc*. 2018;69:437–445.
- [42] Mitchell JA, Ali F, Bailey L, Moreno L, Harrington LS. Role of nitric oxide and prostacyclin as vasoactive hormones released by the endothelium. *Exp Physiol*. 2008;93:141-7.

- [43] Nava E, Llorens S. The Local Regulation of Vascular Function: From an Inside-Outside to an Outside-Inside Model. *Front Physiol.* 2019;10:729.
- [44] Ally AI, Horrobin DF. Thromboxane A2 in blood vessel walls and its physiological significance: relevance to thrombosis and hypertension. *Prostaglandins Med.* 1980;4(6):431-8.
- [45] Görög P, Schraufstatter J, Born GVR. Effect of removing sialic acids from endothelium on the adherence of circulating platelets in arteries in vivo. *Proc. R. Soc. Lond.* 1982;214:471–480.
- [46] Wang Y, Gallant RC, Ni H. Extracellular matrix proteins in the regulation of thrombus formation. *Curr Opin Hematol.* 2016;23(3):280-7.
- [47] Anadol R, Gori T. The mechanisms of late scaffold thrombosis. *Clin Hemorheol Microcirc.* 2017;67(3-4):343-346.
- [48] Nightingale T, Cutler D. The secretion of von Willebrand factor from endothelial cells; an increasingly complicated story. *J Thromb Haemost.* 2013; 11(Suppl 1):192–201.
- [49] Rondaij MG, Bierings R, van Agtmaal EL, Gijzen KA, Sellink E, Kragt A, Ferguson SS, Mertens K, Hannah MJ, van Mourik JA, Fernandez-Borja M, Voorberg J. Guanine exchange factor RalGDS mediates exocytosis of Weibel-Palade bodies from endothelial cells. *Blood.* 2008;112(1):56-63.
- [50] Braune S, Groß M, Walter M, Zhou S, Dietze S, Rutschow S, Lendlein A, Tschöpe C, Jung F. Adhesion and activation of platelets from subjects with coronary artery disease and apparently healthy individuals on biomaterials. *J Biomed Mater Res B Appl Biomater.* 2016;104(1):210-7.

- [51] Reinthaler M, Braune S, Lendlein A, Landmesser U, Jung F. Platelets and coronary artery disease: Interactions with the blood vessel wall and cardiovascular devices. *Biointerphases*. 2016;11(2):029702.
- [52] De Ceunynck K, De Meyer SF, Vanhoorelbeke K. Unwinding the von Willebrand factor strings puzzle. *Blood* 2013; 121:270–7.
- [53] Szántó T, Joutsu-Korhonen L, Deckmyn H, Lassila R. New insights into von Willebrand disease and platelet function. *Semin Thromb Hemost*. 2012;38(1):55-63.
- [54] Nakahata N. Thromboxane A2: physiology/pathophysiology, cellular signal transduction and pharmacology. *Pharmacol Ther*. 2018;118(1):18-35.
- [55] Rickles FR, Edwards RL. Activation of blood coagulation in cancer: Trousseau's Syndrome revisited. *Blood*. 1983;62:14-31.
- [56] Schuetze SM, Zhao L, Chugh R, Thomas DG, Lucas DR, Metko G, Zalupski MM, Baker LH. Results of a phase II study of sirolimus and cyclophosphamide in patients with advanced sarcoma. *Eur J Cancer*. 2012;48(9):1347-53.

## Supplements

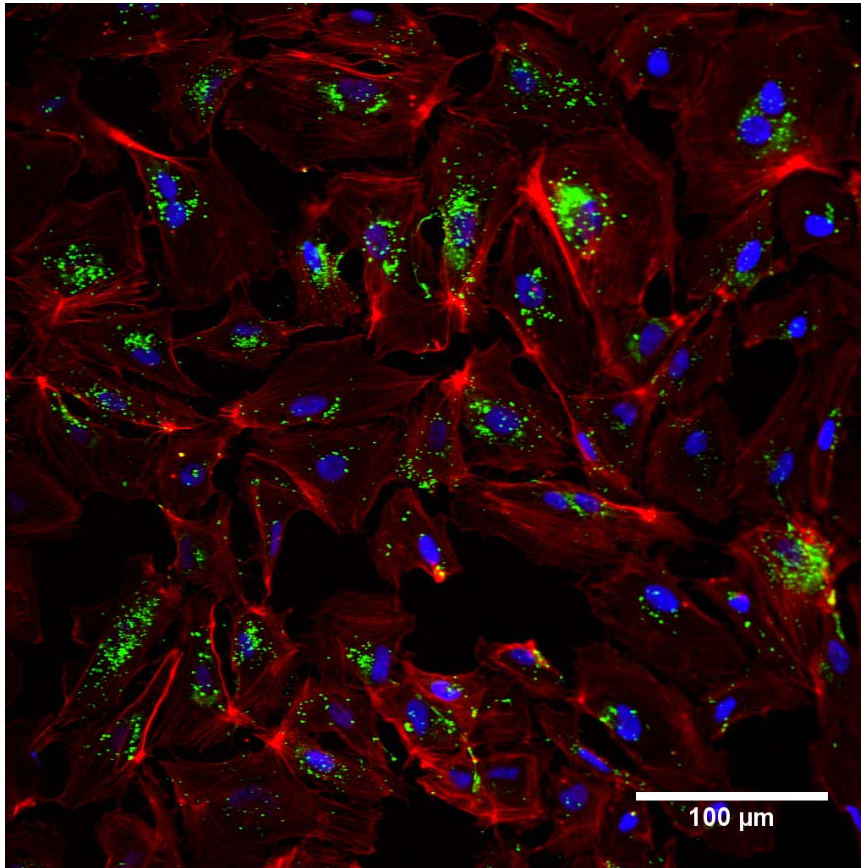


**Figure S1:** Actin and von Willebrand (vWF) expression in adherent untreated human umbilical vein endothelial cells (HUVEC) three days after seeding. Actin is stained in red, vWF in green, nuclei in blue. Images were acquired by confocal laser scanning microscopy (20-fold magnification).